Radiology: Artificial Intelligence

DATA RESOURCES

WAW-TACE: A Hepatocellular Carcinoma Multiphase CT Dataset with Segmentations, Radiomics Features, and Clinical Data

Krzysztof Bartnik, MD, PhD • Tomasz Bartczak, MSc • Mateusz Krzyziński, MSc • Krzysztof Korzeniowski, MD • Krzysztof Lamparski, MD • Piotr Węgrzyn, MD • Eric Lam, MSc • Mateusz Bartkowiak, MD • Tadeusz Wróblewski, MD • Katarzyna Mech, MD • Magdalena Januszewicz, MD • Przemysław Biecek, PhD, MSc, BEng

From the Second Department of Radiology (K.B., K.K., K.L., P.W., M.J.), Department of General, Transplant and Liver Surgery (M.B., T.W.), and Department of General, Gastroenterological and Oncological Surgery (K.M.), Medical University of Warsaw, Banacha 1a, 02-097 Warsaw, Poland; Faculty of Mathematics and Information Science, Warsaw University of Technology, Warsaw, Poland (T.B., M.K., P.B.); and Ottawa Hospital Research Institute, Ottawa, Canada (E.L.). Received May 13, 2024; revision requested July 9; revision received August 30; accepted October 10. **Address correspondence to** K.B. (email: *krzysztof.bartnik@wum.edu.pl*).

Supported by the Medical University of Warsaw and the Warsaw University of Technology under collaborative grant "Integra WUM-PW" (no. 1W12/INTEGRA.1.6/N/23) and carried out with the support of the Laboratory of Bioinformatics and Computational Genomics and the High Performance Computing Center of the Faculty of Mathematics and Information Science Warsaw University of Technology.

Conflicts of interest are listed at the end of this article.

See also commentary by Bitar and Chapiro in this issue.

Supplemental material is available for this article.

Radiology: Artificial Intelligence 2024; 6(6):e240296 • https://doi.org/10.1148/ryai.240296 • Content codes: GI OI AI

Hepatocellular carcinoma (HCC) is the most prevalent primary liver malignancy, encompassing a heterogeneous group of patients with varying prognoses (1). Managing HCC includes various therapeutic options, such as liver transplantation, liver resection, local-regional therapies, chemotherapy and immunotherapy (2). Currently, transarterial chemoembolization (TACE) is the treatment of choice for patients with unresectable HCC without extrahepatic spread and patent venous vessels. Artificial intelligence (AI) research in HCC is evolving rapidly, including use of models to enhance HCC detection, segmentation, and prognostication. Development of such models requires comprehensive data, including imaging and clinical variables (3–5). However, the majority of these studies use internal datasets that are not publicly available alongside the manuscripts and thus lack external data for model validation or performance tuning (6–8). Moreover, existing publicly available datasets have a limited number of cases with imaging and clinical data or tumor segmentations, which are crucial for AI research purposes (9,10). Substantial efforts are being made to provide these data to enhance HCC research.

Here, we present the annotated WAW-TACE dataset, which includes data from patients with HCC treated with TACE at the Medical University of Warsaw (hereafter, MUW), offering an important data resource for diverse researchers. This dataset consists of extensive baseline clinical data, pre-TACE multiphase CT imaging with segmentation masks of HCC lesions and multiple anatomic structures, radiologic therapy response assessments, and crucial patient time-dependent outcome measures such as overall survival (OS), progression-free survival (PFS), and time to favorable treatment response.

Materials and Methods

This retrospective dataset includes 233 treatment-naive patients diagnosed with unresectable HCC and treated with TACE at the Central Clinical Hospital of the MUW between May 2016 and April 2021. The study was approved by the Bioethics Committee at the MUW (decision no. AKBE/41/2024). Figure 1 provides an overview of patient inclusion criteria, the size of the cohort, and the components of the dataset.

The inclusion criteria were: *(a)* at least one HCC lesion; *(b)* patients receiving conventional TACE treatment; *(c)* satisfactory liver function (Child-Pugh class A or B) with no evidence of metastatic disease; and *(d)* the availability of contrast-enhanced CT prior to the first TACE treatment.

Exclusion criteria were: *(a)* patients undergoing liver transplantation, resection, ablation, or drug-eluting beads TACE before or during the follow-up period; *(b)* history of malignant neoplasms other than HCC; *(c)* metastatic disease; *(d)* large vessel invasion; and *(e)* patients with known uncontrolled functional or metabolic diseases that could potentially bias survival (such as myocardial infarction or stroke).

Clinical Data

Pre-TACE clinical assessment.— The diagnosis of HCC was made using imaging criteria (LR-5 according to the Liver Reporting Imaging and Data System [LI-RADS] version 2018) or pathomorphologic examination in patients without concurrent LR-5 observations (considered as equivocal cases, $n = 9$) (3). All patients underwent a series of baseline examinations, and the following variables were collected: age, sex, underlying etiology of chronic liver disease, number of HCC lesions, lesion location, lesion diameter, LI-RADS category, initial treatment response category, and serum levels of total bilirubin, albumin, creatinine, international normalized ratio, α-fetoprotein, and alanine transaminase. Additionally, the following clinical scores were calculated: Barcelona Clinic Liver Cancer stage, Child-Pugh score, hepatoma arterial-embolization prognostic score (11), modified hepatoma arterial embolization prognostic II score (12), six and twelve score (13), and albumin-bilirubin transarterial embolization score (14).

TACE technique and postprocedural follow-up.— All patients underwent standard conventional TACE procedures. Target HCC-feeding vessels were catheterized using a microcatheter, and an injection of 20–40 mL of a lipiodol and doxorubicin mixture in a 1:1 ratio was performed, followed by gelfoam injection until arterial flow stasis was observed.

Abbreviations

AI = artificial intelligence, HCC = hepatocellular carcinoma, LI-RADS = Liver Reporting Imaging and Data System, OS = overall survival, PFS = progression-free survival, TACE = transarterial chemoembolization, VOI = volume of interest

Summary

The WAW-TACE dataset contains baseline multiphase abdominal CT images from 233 treatment-naive patients with hepatocellular carcinoma treated with transarterial chemoembolization and includes 377 handcrafted liver tumor masks, automated segmentations of multiple internal organs, extracted radiomics features, and corresponding extensive clinical data. The dataset can be accessed at *https://zenodo.org/records/12741586*.

Keywords

Liver, Oncology, Hepatocellular Carcinoma

The TACE was repeated after 4 to 6 weeks, as necessary and feasible. Typically, a standard embolization cycle included two (or three, if warranted) TACE sessions, followed by a subsequent CT assessment. Patients showing a favorable treatment response without viable tumor tissue underwent follow-up via serial CT or MRI and serum α-fetoprotein concentration measurements. The detection of viable tumor tissue during follow-up prompted a multidisciplinary team meeting to determine further treatment options.

The index day was set as the date of the first TACE. The end of the follow-up period was specified as the time of death or the last clinical follow-up. For the subgroup demonstrating a LI-RADS nonviable treatment response, the PFS was calculated as the duration between achieving a nonviable response and the reported progression date. Progression was determined by reevaluating post-TACE images (CT or MRI based on availability) for the presence of disease recurrence (according to LI-RADS guidelines) (3).

CT Imaging and Data Processing

CT protocol.— All patients underwent multiphasic CT within 90 days before the initial TACE cycle. A detailed list of information regarding CT scanners, acquisition parameters, and available examination phases is presented in Table 1.

Volume of interest segmentation.— The exact section thicknesses for each individual study is reported in a separate column in the accompanying ct_hcc_metadata file. Each CT examination underwent de-identification and was converted to NIfTI format. No additional filtering or CT image normalization was performed.

The segmentation masks for internal organs were generated using the nnU-Net deep learning model TotalSegmentator (15,16). This algorithm enables the unsupervised segmentation of volumes of interest (VOIs), such as the liver, spleen, and kidneys, among others. For all segmentation tasks, we utilized the pretrained model. No additional training was conducted, as we employed the default hyperparameters as previously described by Wasserthal et al (16). In our dataset, native, arterial, portal, and delayed phases were separately segmented, each with 104 VOIs.

Additionally, for the segmentation of HCC lesions, the TotalSegmentator extension was employed. These VOIs were manually corrected in Slicer 3D software (version 5.4.0) by a radiologist (K.B., with 6 years of overall experience, including 2 years specifically in medical image segmentation) (17). Two independent radiologists conducted validations and made the necessary modifications (K.K. and K.L., with 14 and 11 years of experience in TACE and abdominal radiology, respectively). All observers adhered to a uniform protocol for HCC segmentation, which involved outlining the tumor boundaries on subsequent axial CT sections. These were then connected using the "fill between sections" option with subsequent mask's smoothing using a 3-mm Gaussian filter.

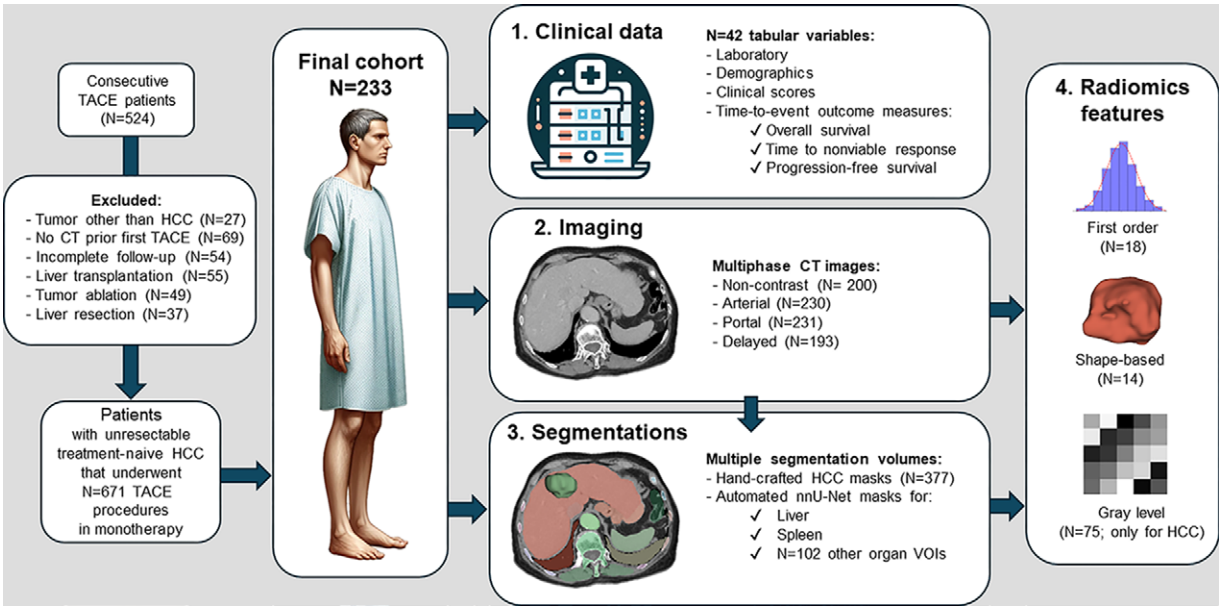

Figure 1: Diagram of patient flowchart and dataset specifications. HCC = hepatocellular carcinoma, TACE = transarterial chemoembolization, VOI = volume of interest.

Table 1: Details of CT Imaging Phases, Scanners, and Acquisition Parameters

Variable		
A: CT Imaging Phase		
Study Phase	Acquisition Time	No. of Series
Native (P0)	No contrast material	200
Late Arterial (P1)	15–30 seconds (after contrast material bolus)	230
Portal Venous (P2)	60–75 seconds	231
Delayed (P3)	4–5 minutes	193
B: CT Scanner		
CT System	Manufacturer and Location	No. of Examinations
Optima CT600	General Electric HealthCare	160
Somatom Xceed	Siemens Healthcare	33
Ingenuity Core	Philips Healthcare	20
Aquilion One	Toshiba Medical Systems	20
C: CT Acquisition Parameters		
CT Parameter	Value	
Section thickness per phase (median)	1.5 mm for arterial; 1.5 mm for portal; 1.25 mm for delayed	
Axial dimension	Matrix of 512 × 512 (for 99% of CT series; *n* = 4 series were 768 × 768)	…
Tube voltage	120 kVp (for 214/233 CT examinations), 100–140 kVp for remaining	…
Tube current	Automated modulation ranging from 250 to 300 mA	…
Reconstruction algorithm	Standard soft tissue kernel	…

Table 2: Baseline Characteristics of Patients Included in the WAW-TACE Dataset

Variable	No. of Patients (*n* = 233)
Age (y)	66 (28–86)
Sex	
Female	48 (20.6)
Male	185 (79.4)
Etiology of chronic liver disease	
Viral	114 (48.9)
Alcoholic	86 (36.9)
Other	33 (14.2)
Child-Turcotte-Pugh class	
A	207 (88.8)
B	26 (11.2)
No. of lesions	
1	149 (63.9)
2	48 (20.6)
3	21 (9.0)
>3	15 (6.4)
Lesion size	
<3 cm	57 (24.5)
3–5 cm	76 (32.6)
>5 cm	100 (42.9)
No. of TACE procedures	
1	21 (9.0)
2	117 (50.2)
3	30 (12.9)
>3	93 (39.9)

Note.—Data are numbers of patients with percentages in parentheses, or medians with ranges in parentheses. TACE = transarterial chemoembolization.

Feature extraction.— We used PyRadiomics (version 3.0.1) to extract features categorized into classes, ensuring adherence to the Imaging Biomarker Standardization Initiative (18). Importantly, all radiomics features were extracted from raw masks generated by TotalSegmentator, without manual VOI correction. For each VOI in the native, late arterial, portal venous, and delayed CT examination phases, there were 32 features belonging to two groups: shape-based features (*n* = 14) and first-order statistics (*n* = 18). Furthermore, from the largest liver tumor VOI, an additional 75 gray-level radiomics features were extracted, including 24 gray-level co-occurrence matrix; 14 gray-level dependence matrix; 16 gray-level size zone matrix; 16 gray-level run length matrix; and five neighboring gray-tone difference matrix.

Results

The WAT-TACE dataset can be downloaded *(https://zenodo.org/records/12741586)* and includes four major components, as outlined in Figure 1: clinical data, imaging, segmentations, and radiomics features.

Clinical Data

Clinical variables, including outcome measures for the patients, are presented in tabular format in a separate file ("clinical_data"). Table S1 presents all headers from the clinical data spreadsheet and variables' definitions. The baseline characteristics of the 233 patients (median age, 66 years (range: 28–86 years); 185 male, 48 female) included in the dataset are summarized in Table 2. The median OS was 27.3 months, with 65 censored patients (27.9%) and a minimum follow-up duration of 33.8 months for surviving patients. The median PFS was 17.7 months, with 60 observed events and 55 censored patients.

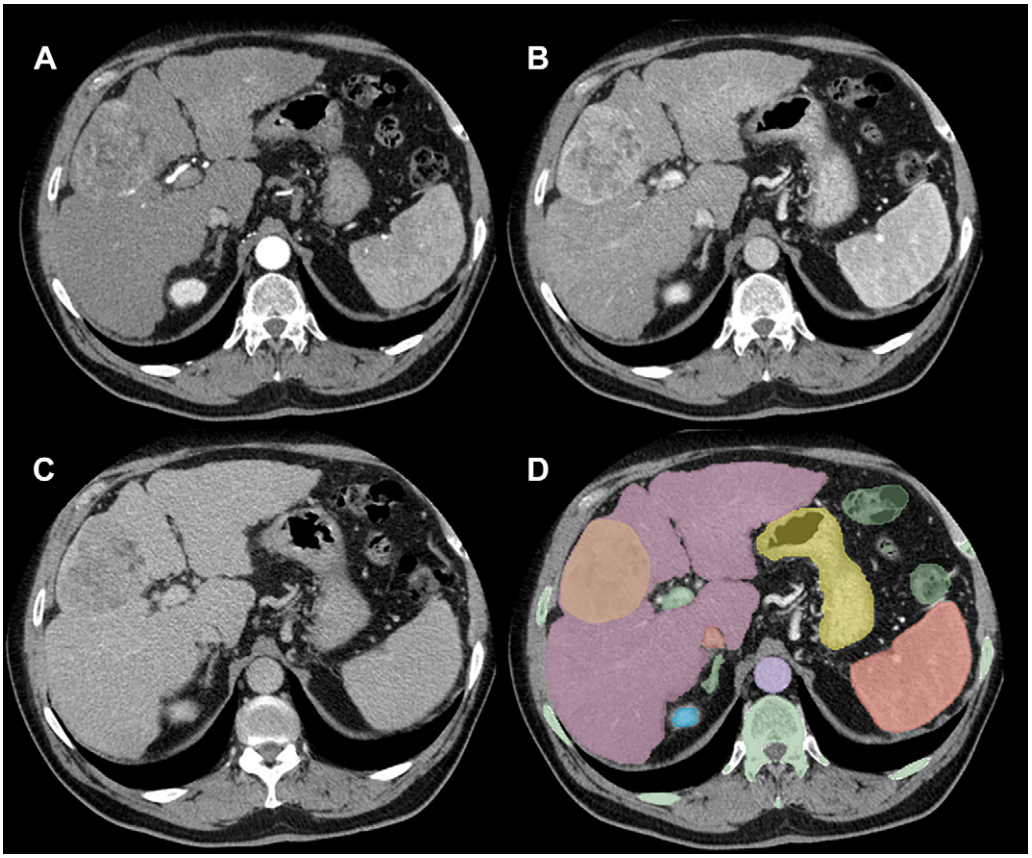

Figure 2: Visual representations of sample axial contrast-enhanced CT images and segmentations: **(A)** arterial phase, **(B)** portal venous phase, **(C)** delayed phase, and **(D)** segmented tumor with multiple organ masks, respectively.

Imaging

In total, the following numbers of CT examinations for each study phase are available in files "ct_scans": precontrast phase (*n* = 200), late arterial phase (*n* = 230), portal venous phase (*n* = 231), and delayed phase (*n* = 193).

Segmentations

The WAW-TACE dataset collectively contains 377 HCC lesion segmentations and 104 organ VOIs per patient, available in files "tumor_masks" and "organ_masks," respectively. A representative set of segmented images from a single WAW-TACE patient is presented in Figure 2. Additional examples of segmented images are presented in Figure 3.

Radiomics Features

The extraction process yielded 3339 radiomic features collectively for all VOIs per patient. These features are listed in tabular form in the "radiomics_data" file.

Discussion

In the expanding era of AI-based research in oncologic imaging, there is a growing demand for extensive data to facilitate the development of prediction models and enhance their generalizability. The WAW-TACE dataset substantially expands the number of publicly accessible annotated HCC lesions imaged using CT, facilitating clinical as well as AI research aimed at predicting time-dependent treatment outcomes. The comprehensive nature of this dataset positions it as an important resource for various researchers.

Our collection adds a substantial amount of annotated data to another recently published TACE dataset (9). In comparison, we also include patients with multiple HCC lesions, not just single tumors. This approach reflects more closely the clinical context of TACE treatments. Moreover, the inclusion of multiphase CT examinations, multiple organ segmentation masks, radiomics features, and comprehensive clinical data combined with time-dependent outcome measures provides a new opportunity for researchers to explore the potential use of AI models. The dataset facilitates robust model training by providing a large, diverse collection of annotated HCC lesions, which is required for developing AI models that can accurately detect and segment tumors. These models can then be used to improve clinical decision-making by providing precise and reliable predictions about disease progression, response to treatments such as TACE, or survival. For example, a part of this dataset was used in a recent study where we used radiomics for TACE outcome prediction, relying solely on automated segmentations (19). Furthermore, the WAW-TACE dataset allows for interinstitutional comparisons and cross-validation, enabling researchers from various institutions to evaluate and test their models against current standards. This can lead to enhanced model performance and generalizability, as models trained and tested on diverse datasets are more likely to perform well across patient populations and imaging conditions. In addition, the manually created HCC segmentation masks can be used to investigate and tailor AI algorithms for tumor segmentation and classification. The dataset reflects the complexity of clinical scenarios by including a variety of cases with multiple lesions, allowing for the development of AI tools capable of addressing

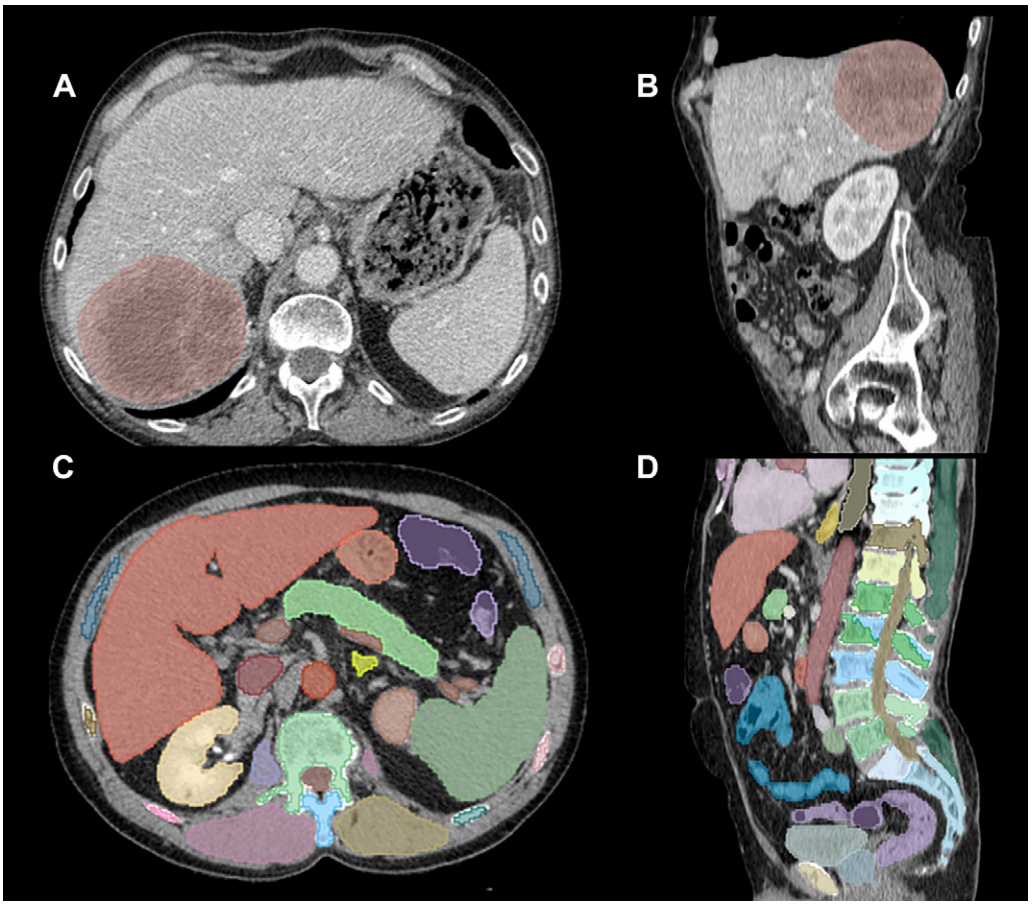

Figure 3: Additional visual examples of segmented contrast-enhanced CT images: manual tumor segmentations in the axial and sagittal planes, respectively **(A, B)**, and deep learning organ volumes of interest in the axial and sagittal planes, respectively **(C, D)**.

real-world challenges in oncologic imaging. Finally, the dataset's extensive clinical data can aid research into personalized medicine. The models trained on this dataset can be used to predict individual patient outcomes by optimizing treatment plans based on tumor characteristics and patient profiles.

There are several limitations worth mentioning. First, only baseline imaging is available in the dataset. Informative image features that may appear on postprocedural scans, or through the assessment of changes over time, cannot be evaluated with this dataset. Second, not all patients included have all CT phase series available, leading to some missing image data. Furthermore, the imaging data comes from different CT systems and the median section thicknesses varied between patients, which should be emphasized when using the data for radiomics analysis. Notably, no specific CT image preprocessing or resampling was performed prior to radiomics feature extraction. Finally, the most reliable study end point was OS, recorded objectively using the national government database. However, TACE treatment response assessments and PFS were more subjective, relying on the reevaluation of post-TACE imaging by one author (K.B.). The process involved using the LI-RADS treatment response algorithm, cross-referencing imaging with clinical data, radiology reports, and laboratory data. Despite these measures, the subjective nature of response evaluation may introduce some variability.

In summary, this interdisciplinary resource is an important contribution to HCC research and facilitates use of AI in medical imaging research aimed at enhancing patient outcomes.

Author contributions: Guarantor of integrity of entire study, **K.B.**; study concepts/study design or data acquisition or data analysis/interpretation, all authors; manuscript drafting or manuscript revision for important intellectual content, all authors; approval of final version of submitted manuscript, all authors; agrees to ensure any questions related to the work are appropriately resolved, all authors; literature research, **K.B., K.L., T.W.**; clinical studies, **K.B., K.K., K.L., M.B., T.W.**; experimental studies, **K.B., T.B., P.W., M.B., T.W.**; statistical analysis, **K.B., T.B., M.K.**; and manuscript editing, **K.B., T.B., M.K., K.K., P.W., E.L., M.B., T.W., K.M., M.J., P.B.**

Data sharing statement: Data generated by the authors or analyzed during the study are available at *https://zenodo.org/records/11063785*. Researchers interested in utilizing this dataset can use it for scientific research purposes only. Access to this dataset is not contingent upon the requirement for co-authorship or the establishment of a research collaboration.

Disclosures of conflicts of interest: K.B. No relevant relationships. **T.B.** Support, Politechnika Warszawska. **M.K.** No relevant relationships. **K.K.** No relevant relationships. **K.L.** No relevant relationships. **P.W.** Support, Medical University of Warsaw, Warsaw University of Technology. **E.L.** No relevant relationships. **M.B.** No relevant relationships. **T.W.** No relevant relationships. **K.M.** No relevant relationships. **M.J.** No relevant relationships. **P.B.** No relevant relationships.

References

1. Marrero JA, Kulik LM, Sirlin CB, et al. Diagnosis, Staging, and Management of Hepatocellular Carcinoma: 2018 Practice Guidance by the American Association for the Study of Liver Diseases. Hepatology 2018;68(2):723–750.
2. Heimbach JK, Kulik LM, Finn RS, et al. AASLD guidelines for the treatment of hepatocellular carcinoma. Hepatology 2018;67(1):358–380.
3. Chernyak V, Fowler KJ, Kamaya A, et al. Liver Imaging Reporting and Data System (LI-RADS) Version 2018: Imaging of Hepatocellular Carcinoma in At-Risk Patients. Radiology 2018;289(3):816–830.
4. Pellat A, Barat M, Coriat R, Soyer P, Dohan A. Artificial intelligence: A review of current applications in hepatocellular carcinoma imaging. Diagn Interv Imaging 2023;104(1):24–36.

5. Calderaro J, Seraphin TP, Luedde T, Simon TG. Artificial intelligence for the prevention and clinical management of hepatocellular carcinoma. J Hepatol 2022;76(6):1348–1361.
6. Morshid A, Elsayes KM, Khalaf AM, et al. A machine learning model to predict hepatocellular carcinoma response to transcatheter arterial chemoembolization. Radiol Artif Intell 2019;1(5):e180021.
7. Bernatz S, Elenberger O, Ackermann J, et al. CT-radiomics and clinical risk scores for response and overall survival prognostication in TACE HCC patients. Sci Rep 2023;13(1):533.
8. Bera K, Braman N, Gupta A, Velcheti V, Madabhushi A. Predicting cancer outcomes with radiomics and artificial intelligence in radiology. Nat Rev Clin Oncol 2022;19(2):132–146.
9. Moawad AW, Morshid A, Khalaf AM, et al. Multimodality annotated hepatocellular carcinoma data set including pre- and post-TACE with imaging segmentation. Sci Data 2023;10(1):33.
10. Erickson BJ, Kirk S, Lee Y, et al. The Cancer Genome Atlas Liver Hepatocellular Carcinoma Collection (TCGA-LIHC) (Version 5). The Cancer Imaging Archive. https://doi.org/10.7937/K9/TCIA.2016.IMMQW8UQ. Published 2016. Updated May 2020. Accessed May 2024.
11. Kadalayil L, Benini R, Pallan L, et al. A simple prognostic scoring system for patients receiving transarterial embolisation for hepatocellular cancer. Ann Oncol 2013;24(10):2565–2570.
12. Park Y, Kim SU, Kim BK, et al. Addition of tumor multiplicity improves the prognostic performance of the hepatoma arterial-embolization prognostic score. Liver Int 2016;36(1):100–107.
13. Wang Q, Xia D, Bai W, et al. Development of a prognostic score for recommended TACE candidates with hepatocellular carcinoma: A multicentre observational study. J Hepatol 2019;70(5):893–903.
14. Lee IC, Hung YW, Liu CA, et al. A new ALBI-based model to predict survival after transarterial chemoembolization for BCLC stage B hepatocellular carcinoma. Liver Int 2019;39(9):1704–1712.
15. Isensee F, Jaeger PF, Kohl SAA, Petersen J, Maier-Hein KH. nnU-Net: a self-configuring method for deep learning-based biomedical image segmentation. Nat Methods 2021;18(2):203–211.
16. Wasserthal J, Breit HC, Meyer MT, et al. TotalSegmentator: Robust Segmentation of 104 Anatomic Structures in CT Images. Radiol Artif Intell 2023;5(5):e230024.
17. Fedorov A, Beichel R, Kalpathy-Cramer J, et al. 3D Slicer as an image computing platform for the Quantitative Imaging Network. Magn Reson Imaging 2012;30(9):1323–1341.
18. Zwanenburg A, Vallières M, Abdalah MA, et al. The Image Biomarker Standardization Initiative: Standardized Quantitative Radiomics for High-Throughput Image-based Phenotyping. Radiology 2020;295(2):328–338.
19. Bartnik K, Krzyziński M, Bartczak T, et al. A novel radiomics approach for predicting TACE outcomes in hepatocellular carcinoma patients using deep learning for multi-organ segmentation. Sci Rep 2024;14(1):14779.